University of New Orleans

ScholarWorks@UNO

Physics Faculty Publications

Department of Physics

2000

Causal implications of viscous damping in compressible fluid flows

P. M. Jordan

Martin R. Meyer
University of New Orleans

Ashok Puri
University of New Orleans

Causal implications of viscous damping in compressible fluid flows

P. M. Jordan,[1] Martin R. Meyer,[2] and Ashok Puri[2,*]

[1]*Code 7181, Naval Research Laboratory, Stennis Space Center, Mississippi 39529*
[2]*Department of Physics, University of New Orleans, New Orleans, Louisiana 70148*
(Received 20 December 1999; revised manuscript received April 25 2000)

Classically, a compressible, isothermal, viscous fluid is regarded as a mathematical continuum and its motion is governed by the linearized continuity, Navier-Stokes, and state equations. Unfortunately, solutions of this system are of a diffusive nature and hence do not satisfy causality. However, in the case of a half-space of fluid set to motion by a harmonically vibrating plate the classical equation of motion can, under suitable conditions, be approximated by the damped wave equation. Since this equation is hyperbolic, the resulting solutions satisfy causal requirements. In this work the Laplace transform and other analytical and numerical tools are used to investigate this apparent contradiction. To this end the exact solutions, as well as their special and limiting cases, are found and compared for the two models. The effects of the physical parameters on the solutions and associated quantities are also studied. It is shown that propagating wave fronts are only possible under the hyperbolic model and that the concept of phase speed has different meanings in the two formulations. In addition, discontinuities and shock waves are noted and a physical system is modeled under both formulations. Overall, it is shown that the hyperbolic form gives a more realistic description of the physical problem than does the classical theory. Lastly, a simple mechanical analog is given and connections to viscoelastic fluids are noted. In particular, the research presented here supports the notion that linear compressible, isothermal, viscous fluids can, at least in terms of causality, be better characterized as a type of viscoelastic fluid.

PACS number(s): 47.40.−x, 02.30.Jr, 43.20.+g, 47.10.+g

I. INTRODUCTION

In the classical theory of fluids, the propagation of small-amplitude longitudinal waves in a compressible, isothermal, viscous fluid is governed by the linearized continuity, Navier-Stokes, and state equations (see Kinsler *et al.* [1])

$$\frac{\partial p}{\partial t} + \rho_0 c^2 \boldsymbol{\nabla} \cdot \mathbf{v} = 0, \tag{1.1}$$

$$\rho_0 \frac{\partial \mathbf{v}}{\partial t} = -\boldsymbol{\nabla} p + \left(\frac{4\mu}{3} + \eta_B \right) \boldsymbol{\nabla}(\boldsymbol{\nabla} \cdot \mathbf{v}), \tag{1.2}$$

$$p = c^2(\rho - \rho_0), \tag{1.3}$$

where $\mathbf{v}$ is the velocity vector, p is the pressure, ρ is the density, the constants $\mu, \eta_B, \rho_0, c > 0$ are the shear viscosity, bulk viscosity, ambient density, and sound speed, respectively, and of course the flow is irrotational (i.e., $\boldsymbol{\nabla} \times \mathbf{v} = \mathbf{0}$). Guided by Kinsler *et al.* [1], and using the well-known tools of vector calculus, the above system can be written as the third-order partial differential equation (PDE)

$$c^2 \nabla^2 u - \frac{\partial^2 u}{\partial t^2} + \frac{4\mu}{3\rho_0} \frac{\partial(\nabla^2 u)}{\partial t} = 0, \tag{1.4}$$

where u is a component of $\mathbf{v}$ and the Stokes assumption (i.e., $\eta_B = 0$) has been made. Initial-boundary value problems (IBVP's) involving the one-dimensional form of this equa-

tion have been solved and analyzed by Blackstock [2] and Norwood [3]. It is of interest to note that in its one- (two-) dimensional form Eq. (1.4) is, with the appropriate coefficients, the equation of motion of a string (membrane) with internal damping [4] and also describes the motion of a viscoelastic fluid under the Kelvin-Voit body model [5].

Now, consider the case of an initially quiescent half-space of fluid set to motion by an infinite, harmonically vibrating bounding plate (i.e., the compressible fluid analogy of the transient form of Stokes's second problem [6]). We observe that for sufficiently large $t > 0$ [more precisely $t \gg 4\mu/(3\rho_0 c^2)$, see Sec. III D], the time dependence of u will be (approximately) solely of the form $e^{i\omega t}$, where $\omega > 0$ is the constant vibration frequency of the bounding plate. Thus we have

$$\nabla^2 u \approx -\frac{\omega^2}{c^2} \left(\frac{u}{1 + 4i\omega\mu/(3\mu_0 c^2)} \right). \tag{1.5a}$$

Moreover, for many fluids (e.g., air, water) the coefficient of the mixed derivative damping term in Eq. (1.4) is a very small quantity. Hence, following McLachlan [7], we can regard the mixed derivative term in Eq. (1.4) as a sink and, so as to obtain a wave equation with an alternate form of damping while maintaining a well-posed IBVP, approximate only its Laplacian part, when $\omega \ll 3\rho_0 c^2/(4\mu)$ (a condition easily satisfied in most, if not all, classical fluids over virtually the entire frequency spectrum of acoustical applications), by

$$\nabla^2 u \approx -\frac{\omega^2}{c^2} u. \tag{1.5b}$$

Using Eq. (1.5b), Eq. (1.4) becomes approximately

---

*Author to whom correspondence should be addressed. Electronic address: apuri@uno.edu

$$c^2 \nabla^2 u - \frac{\partial^2 u}{\partial t^2} - \frac{4\mu\omega^2}{3\rho_0 c^2} \frac{\partial u}{\partial t} = 0, \qquad (1.6)$$

where c is now identified as the phase speed. Equation (1.6), a hyperbolic PDE, is a special case of the telegraph equation known as the damped wave equation. As is well known, this equation describes a vast array of physical systems. For example, the damped wave equation governs the propagation of ''second sound'' (i.e., thermal waves) in a thermally conducting medium where the heat flux vector is given by the Maxwell-Cattaneo equation [8], the propagation of electromagnetic waves in an electrically conducting medium (see, e.g., Born and Wolf [9]), the migration dynamics of fish schools [10], the random walk problem [11], the motion of a string or membrane with external damping (see, e.g., Morse and Feshbach [12]), and it is the equation of motion of a viscoelastic fluid under the Maxwell body theory [5].

In this work we demonstrate, as was noted earlier by Blackstok [2], that solutions of the classical equation of motion for this problem do not satisfy causality [13]. We also consider solutions of the approximate hyperbolic formulation of the problem as alternatives that do satisfy casualty. In an effort to resolve this contradiction and to provide a deeper physical insight into this problem we present the following: A comparative study of the one-dimensional form of these two models [i.e., the classical model corresponding to Eq. (1.4) and the approximate hyperbolic formulation described by Eq. (1.6)], an examination of their special and/or limiting cases, and a study of the roles of the various quantities of interest (e.g., the constant c has different physical interpretations in the two formulations). In effect, we show that the approximate hyperbolic form gives an overall more realistic description of the physical problem than does the classical theory. Moreover, we also point out that the hyperbolic formulation of the problem actually suggests that classical fluids described in this work are, at least in terms of causality, better modeled as viscoelastic fluids of the Maxwell type.

To this end, we present in Sec. II the exact solutions for both the classical and hyperbolic formulations found using the temporal Laplace transform. In Sec. III we present a variety of analytical results: a number of special and/or limiting cases are considered, several associated physical quantities are given, and a (possible) new definite integral, found serendipitously in the course of this investigation, is presented. Section IV contains numerical results for various values of the time and solution parameters, as well as for some of the associated physical quantities, and a physical system is considered. Finally, in Sec. V conclusions are given followed by a brief discussion which, in addition to presenting a simple mechanical analog, highlights the connection between classical and the viscoelastic fluids.

II. MATHEMATICAL ANALYSIS

Taking the positive z axis of a Cartesian coordinate system in the upward direction, let a compressible fluid occupy the half-space $x>0$ adjacent to a flat plate in the yz plane. Initially, both the plate and fluid are at rest. At time $t=0^+$ a flow is induced by the vibration of the plate along the x axis

with velocity $U_0 \cos(\omega t)$ or $U_0 \sin(\omega t)$, where U_0 is a constant. Under these conditions, no flow occurs in the y and z directions and the flow velocity at a given point in the fluid depends only on the x coordinate of the point and the time t. We model the above physical system with the following one-dimensional IBVP:

$$c^2 \frac{\partial^2 u}{\partial x^2} - \frac{\partial^2 u}{\partial t^2} + a^2 \frac{\partial^3 u}{\partial x^2 \partial t} = 0, \quad a>0, \quad x,t>0$$

$$c^2 \frac{\partial^2 u}{\partial x^2} - \frac{\partial^2 u}{\partial t^2} - r \frac{\partial u}{\partial t} = 0, \quad r>0, \quad x,t>0, \qquad (2.1)$$

$$u(0,t)=g(t), \quad u(\infty,t)=0, \quad t>0, \qquad (2.2)$$

$$u(x,0)=u_t(x,0)=0, \quad x>0, \qquad (2.3)$$

where the velocity vector is given by $\mathbf{v}=(u(x,t),0,0)$, $g(t)$ ($\equiv 0$ for $t<0$) takes on the value of $U_0 \cos(\omega t)$ or $U_0 \sin(\omega t)$, and to simplify the notation we have set $a^2 \equiv 4\mu/(3\rho_0)$ and $r \equiv 4\mu\omega^2/(3\rho_0 c^2)$. Applying the temporal Laplace transform $\mathcal{L}[\cdot]$ and solving the resulting ordinary differential equation yields the transform domain solution

$$\bar{u}(x,s)=\mathcal{L}[g(t)] \times \begin{cases} \exp\left(-\dfrac{x}{c}\sqrt{\dfrac{s^2}{1+s/l^2}}\right), & a>0 \\[4mm] \exp\left(-\dfrac{x}{c}\sqrt{s(s+r)}\right), & r>0, \end{cases}$$
$$(2.4)$$

where

$$\mathcal{L}[g(t)]=U_0 \times \begin{cases} \dfrac{s}{s^2+\omega^2}, & g(t)=U_0\cos(\omega t), \\[4mm] \dfrac{\omega}{s^2+\omega^2}, & g(t)=U_0\sin(\omega t), \end{cases}$$
$$(2.5)$$

$l^2 \equiv (c^2/a^2)=3\rho_0 c^2/(4\mu)$, s is the complex transform parameter, and $\bar{u} \equiv \mathcal{L}[u]$. Since the $r>0$ solution can be easily extracted from the $k<0$ case of Eq. (2.7) of Ref. [14] [on setting $b=0$ and $F(t)=g(t)$], we simply give it below. Here, we derive only the xt-domain solution for the $a>0$ case of Eq. (2.4). To this end we note that Eq. (2.4) possesses simple poles at $s=\pm i\omega$ and has a branch point at $s=-l^2$. Having found the singularities, we can now employ the Laplace inversion formula (see, e.g., Churchill [15]). Thus, on integrating along the Bromwich contour Γ (see Fig. 1) in the counterclockwise direction, taking the limits $\epsilon \to 0^+$ and $R \to \infty$, and employing the residue theorem [15] we obtain the complete, exact, xt-domain solution

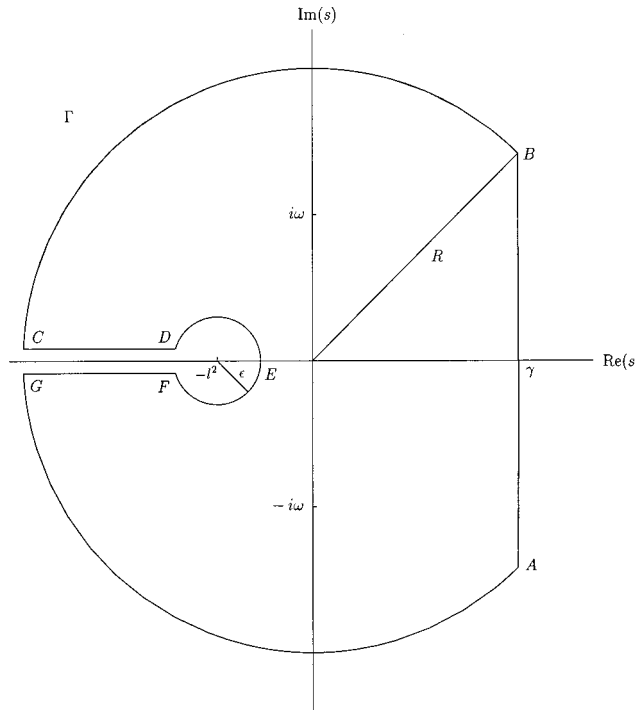FIG. 1. Bromwich contour Γ used in the inversion of the $a>0$ case of Eq. (2.4).

$$u(x,t)=\theta(t)\times\begin{cases}\times\begin{cases}e^{-\alpha_1 x}g(t-\alpha_2 x/\omega)-\dfrac{U_0}{\pi}\displaystyle\int_{l^2}^{\infty}\dfrac{\eta e^{-t\eta}\sin[xh(\eta)]d\eta}{\eta^2+\omega^2}, & g(t)=U_0\cos(\omega t), \quad a>0,\\[3mm] e^{-\alpha_1 x}g(t-\alpha_2 x/\omega)+\dfrac{\omega U_0}{\pi}\displaystyle\int_{l^2}^{\infty}\dfrac{e^{-t\eta}\sin[xh(\eta)]d\eta}{\eta^2+\omega^2}, & g(t)=U_0\sin(\omega t), \quad a>0\end{cases}\\[6mm]\theta(t-x/c)\left(e^{-rx/(2c)}g(t-x/c)+rx\displaystyle\int_{x/c}^{t}g(t-\zeta)K(x,\zeta)d\zeta\right), \quad r>0,\end{cases}$$
(2.6)

where $\theta(\cdot)$ is the Heaviside unit step function,

$$h(\eta)=\frac{\eta}{c\sqrt{\eta/l^2-1}},\quad \alpha_{1,2}=\frac{\omega}{c}\sqrt{\frac{\mp 1+\sqrt{1+\omega^2/l^4}}{2(1+\omega^2/l^4)}},$$
(2.7)

$$K(x,\zeta)=\frac{e^{-r\zeta/2}}{2c}\left(\frac{I_1[(r/2)\sqrt{(\zeta^2-x^2/c^2)}]}{\sqrt{\zeta^2-x^2/c^2}}\right),\quad (2.8)$$

and where $I_n[\ ]$ denotes the modified Bessel function of the first kind of order n.

III. ANALYTICAL RESULTS

In this section we examine the behavior of Eq. (2.6) using analytical techniques. Both small and large time solutions are given. In addition, we derive the relevant wave parameters that characterize the behavior of the solution for large values of time. We also examine the curve structure and determine the amplitudes of the jump discontinuities occurring in u and its first derivatives for the case of $r>0$. Moreover, we note several important aspects of solution (2.6) and we call attention to several of its special and/or limiting cases. Lastly, we present a possible new definite integral found during the course of this research.

A. Small-time behavior

Expanding the transform domain solution [Eq. (2.4)] for large s and then inverting gives us small-time expressions for Eq. (2.6). Thus, for $a>0$ the small-time solutions are given by (see also Refs. [2,3])

$$u(x,t) \approx U_0 \theta(t) \times \begin{cases} P_c(x)\mathrm{erfc}[x/2a\sqrt{t}] + Q_c(x)\sqrt{t/\pi}\, e^{-x^2/(4a^2t)}, & g(t) = U_0 \cos(\omega t) \\ P_s(x,t)\mathrm{erfc}[x/2a\sqrt{t}] - Q_s(x,t)\sqrt{t/\pi}\, e^{-x^2/(4a^2t)}, & g(t) = U_0 \sin(\omega t), \end{cases} \tag{3.1}$$

where $\mathrm{erfc}[\cdot]$ is the complementary error function [15], $x^2 a^{-2} \ll t \ll \mathrm{Min}[\omega^{-1}, l^{-2}]$, and

$$P_c(x) = 1 - \frac{l^2 x^2}{2a^2}, \tag{3.1a}$$

$$P_s(x,t) = \omega\left(t - \frac{l^2 x^2 t}{4a^2} + \frac{x^2}{2a^2}\right), \tag{3.1b}$$

$$Q_c(x) = \frac{l^2 x}{a}, \tag{3.1c}$$

$$Q_s(x,t) = \omega\left(\frac{x}{a} - \frac{2l^2 xt}{3a}\right). \tag{3.1d}$$

For $r>0$ the small-time solutions are [14]

$$u(x,t) \approx U_0 e^{-rx/(2c)} \theta(t-x/c)$$

$$\times \begin{cases} 1 + r^2 x(t-x/c)/(8c), & g(t) = U_0 \cos(\omega t) \\ \omega(t-x/c), & g(t) = U_0 \sin(\omega t), \end{cases} \tag{3.2}$$

where for $xc^{-1} < t \ll \mathrm{Min}[\omega^{-1}, r^{-1}]$. The advantage of Eqs. (3.1) and (3.2) over Eq. (2.6) is that they can be obtained without the need of contour integration and they are much easier to implement numerically. In addition, they give us insight into the behavior of the transient terms. From Eq. (3.1) we see that the small-time behavior will always be of a diffusive character for $a>0$. In addition we see that for every $t>0$, the Heaviside function on the right-hand side of Eq. (3.1) is always unity, indicating that the vibrations occurring at the $x=0$ boundary are felt instantly, but not equally, throughout the entire half space. In contrast, Eq. (3.2) shows that for $r>0$ we have an exponentially damped disturbance propagating in the positive x direction (i.e., away from the plate) with speed c. Finally, we see from Eqs. (3.1) and (3.2) that for $g(t) = U_0 \cos(\omega t)$, u is independent of ω under small-t conditions.

TABLE I. Propagating discontinuities in u, u_t, and u_x.

Case	$a>0$		$r>0$	
Wave front	$x=ct$		$x=ct$	
$g(t)$	$U_0 \cos(\omega t)$	$U_0 \sin(\omega t)$	$U_0 \cos(\omega t)$	$U_0 \sin(\omega t)$
$\mathcal{S}[u]$	0	0	$U_0 e^{-rx/2}$	0
$\mathcal{S}[u_t]$	0	0	∞	$\omega U_0 e^{-rx/2}$
$\mathcal{S}[u_x]$	0	0	∞	$-c\omega U_0 e^{-rx/2}$

B. Discontinuities

In Table I we have listed the amplitudes of the propagating jump discontinuities in u and its first derivatives, as determined using the methods employed by Jordan and Puri [14]. Here $\mathcal{S}[\ ]$, the saltus operator, denotes the jump in a quantity across the plane $x=ct$ (see Ref. [14]). From Table I we see that within the solution domain (i.e., $x,t>0$), u and its first derivatives are continuous for the case $a>0$. Furthermore, it can be easily shown that u is infinitely differentiable with respect to both x and t [i.e., $u \in C^\infty(x,t>0)$] for all admissible g and $a>0$ (see Ref. [14]).

For $r>0$ and $g(t) = U_0 \sin(\omega t)$, u is again a continuous function within its solution domain. However, both u_x and u_t, the first spatial and temporal derivatives of u, respectively, each suffer a finite jump discontinuity across the plane $x=ct$. Hence u is only of class C^0 and thus it follows that u has a corner on $x=ct$. In contrast, taking $g(t) = U_0 \cos(\omega t)$, again for $r>0$, results in u itself experiencing a jump discontinuity across $x=ct$. Physically, of course, this plane represents the wave front. Technically, in the hyperbolic case, the plane $x=ct$ is known as a shock wave, or a singular surface of order zero, for $g(t) = U_0 \cos(\omega t)$ while for $g(t) = U_0 \sin(\omega t)$ it is referred to as an acceleration wave, or a singular surface order one (see, e.g., Truesdell and Toupin [16]). Moreover, we see that the amplitude of every finite, nonzero jump given in Table I decays exponentially over time (since $x=ct$ at the wave front).

In Fig. 2 we have plotted the $r>0$ case of Eq. (2.6) for $g(t) = U_0 \cos(\omega t)$ (solid line) and $g(t) = U_0 \sin(\omega t)$ (bold line). The values of the physical parameters used correspond to air at $0\,^\circ\mathrm{C}$ and were taken from Ref. [1] [Table (b), p. 462]. Observe that ahead of the wave front (i.e., the half-space $x>ct$), $u \equiv 0$ (since the fluid was initially in an undisturbed state), behind it (i.e., the slab $0<x<ct$) lies the region of the solution domain where the effects of the input g have already been felt. In addition, the jump associated with the shock wave resulting from the $U_0 \cos(\omega t)$ boundary data
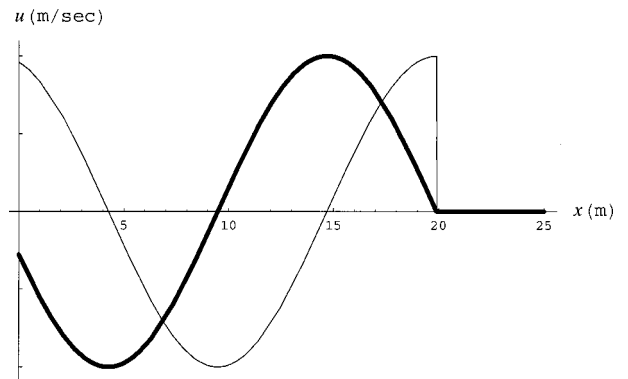
u (m/sec)

FIG. 2. u vs x for air at $0\,^\circ\mathrm{C}$ with $\omega = 100.0$ Hz (giving $r = 1.59 \times 10^{-6}$ sec^{-1}) and $t = 0.06$ sec. Bold line: $g(t) = \sin(\omega t)$; solid line: $g(t) = \cos(\omega t)$.

is clearly visible as well as the corner associated with the $U_0 \sin(\omega t)$ input.

C. Displacement thickness

In classical incompressible fluid theory the displacement thickness δ^* refers to the distance from a flat plate that a streamline in the outer flow is displaced by the presence of viscosity and is defined as

$$\delta^*(t) = U_0^{-1} \int_0^\infty u(x,t)dx. \tag{3.3}$$

In this work, however, the phrase displacement thickness simply refers to the area under the u vs x for some fixed $t>0$. Hence, from Eqs. (2.6) and (3.3) we find

$$\delta^*(t) = U_0^{-1} \theta(t) \times \begin{cases} a\left[M(t) + (l^2/2) \int_0^t e^{-l^2\zeta/2} M(t-\zeta)\{I_0(l^2\zeta/2) + I_1(l^2\zeta/2)\}d\zeta \right], & a>0 \\ c\left[\int_0^t e^{-r\zeta/2} g(t-\zeta) I_0(r\zeta/2)d\zeta \right], & r>0, \end{cases} \tag{3.4}$$

where

$$M(t) = U_0 \sqrt{\frac{2}{\omega}} \times \begin{cases} C(\sqrt{2\omega t/\pi})\cos(\omega t) + S(\sqrt{2\omega t/\pi})\sin(\omega t), & g = U_0\cos(\omega t) \\ C(\sqrt{2\omega t/\pi})\sin(\omega t) - S(\sqrt{2\omega t/\pi})\cos(\omega t), & g = U_0\sin(\omega t), \end{cases} \tag{3.5}$$

and where $C(\ )$ and $S(\ )$ are the Fresnel integrals of the cosine and sine types, respectively. Observe that for $a>0$, δ^* is proportional to a for any fixed positive t while for $r>0$, δ^* is proportional to c, again for any fixed positive t.

D. Special and limiting cases

Returning to Eq. (2.6) we note that as $c\to 0^+$, the (fixed) $a>0$ case of Eq. (2.6) approaches the solution of the heat equation for the corresponding IBVP and, as $r\to 0^+$, the $r>0$ case of Eq. (2.6) approaches $\theta(t-x/c)g(t-x/c)$, the solution of the undamped (or classic) wave equation for the present IBVP. Moreover, we see that for fixed c, $l\to\infty$ as $a\to 0^+$. Consequently, the transient (i.e., integral) terms found in the $a>0$ cases of Eq. (2.6) approach zero (since both limits of integration are approaching infinity), $\alpha_{1,2} \to \{0, \omega/c\}$, and $\theta(t) \to \theta(t-x/c)$ [since the branch point at $s=-l^2$ is tending to $-\infty$ and $\bar{u}(x,s)$ is analytic in the half-plane $\text{Re}(s)>\gamma$]. Thus, as one would expect, $u\to\theta(t-x/c)g(t-x/c)$ as $a\to 0^+$.

Clearly as $t\to\infty$, $u(x,t)\to u_\infty(x,t)$, where

$$u_\infty(x,t) = e^{-\alpha_1 x} g(t - \alpha_2 x/\omega), \quad a>0. \tag{3.6}$$

In a strict sense, $u_\infty(x,t)$ is not the steady-state solution since it contains t explicitly. It is, however, known as the sustained or quasi-steady-state solution. In Table II we list the relevant propagation parameters associated with u_∞ (see also Refs. [2,3]). Here penetration depth refers to the value of x for which the amplitude of u_∞ has decreased to $U_0 e^{-1}$ and wavelength denotes the distance between two successive layers of fluid which vibrate in phase [17].

Expanding $\alpha_{1,2}$ for large frequency we find

$$\alpha_{1,2} \sim \frac{1}{a}\sqrt{\frac{\omega}{2}}, \quad \omega \gg l^2. \tag{3.7}$$

Expanding $\alpha_{1,2}$ for small frequency we find

$$\alpha_1 \approx \frac{a^2\omega^2}{2c^3}, \quad \alpha_2 \approx \frac{\omega}{c}, \quad \omega \ll l^2. \tag{3.8}$$

Thus when ω is very much larger than l^2, u_∞ (approximately) satisfies the classic diffusion equation. For $\omega \ll l^2$, we find that $u_\infty \approx e^{-rx/(2c)} g(t-x/c)$, where again $r = 4\mu\omega^2/(3\rho_0 c^2)$ (i.e., for ω sufficiently small, u_∞ is approximately equal to the nonintegral part of the $r>0$ solution). Thus we see, as illustrated here in the one-dimensional case, that solutions of Eq. (1.4) for the present IBVP are approximately equal to those of Eq. (1.6) when $\omega \ll l^2$ and $(xc^{-1})<t\gg l^{-2}$. Furthermore, when ω is so small that ω^2 can be neglected in comparison to ω, u_∞ approximates the solution to the well-known wave equation. [Clearly so does the $r>0$ case of Eq. (2.6).] Moreover, in terms of the phase velocity v_p we have

$$v_p \sim a\sqrt{2\omega} \quad (\omega \gg l^2), \quad v_p \approx c \quad (\omega \ll l^2). \tag{3.9}$$

From the first of Eqs. (3.9) we find that the propagation medium exhibits anomalous dispersion [18] when ω is large compared to l^2 (i.e., v_p is an increasing function of frequency). However, from the second of Eqs. (3.9) we find that

TABLE II. Propagation parameters.

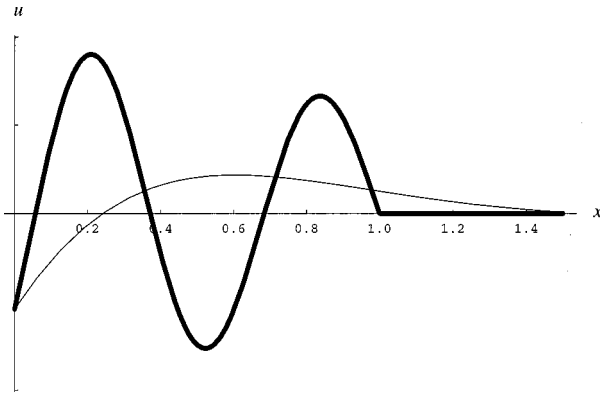| Name	Parameter
Attenuation coefficient	α_1
Penetration depth	$1/\alpha_1$
Wave number	α_2
Phase velocity v_p	ω/α_2
Wavelength	$2\pi/\alpha_2$
Phase lag	$\alpha_2 x$

FIG. 3. u vs x in nondimensional (ND) units for $t=c=r=1.0$ and $\omega=10.0$. Bold line: hyperbolic; solid line: classical.

the propagation medium tends to be nondispersive when ω is much smaller than l^2 (i.e., v_p is a constant, independent of frequency; the medium behaves as does free space with respect to electromagnetic waves [9]). Furthermore, it should be clear that when $r \ll 2c/x$, then the propagation medium is essentially of a nondispersive nature (implying that far away from the plate, the $r>0$ solution behaves very much like that of the classic wave equation).

Taking $g(t)=U_0 e^{i\omega t}$ makes u a complex quantity. McLachlan [7] has given the complex-valued solution for the case $r>0$. For $a>0$, the complex-valued quasi-steady-state solution is

$$\mathcal{U}_\infty(x,t)=U_0 e^{-\alpha_1 x} \exp[i(\omega t-\alpha_2 x)]. \qquad (3.10)$$

The modulus of Eq. (3.10) is easily found to be

$$|\mathcal{U}_\infty(x,t)|=U_0 e^{-\alpha_1 x}. \qquad (3.11)$$

Using the large and small frequency expressions given above, we find that

$$|\mathcal{U}_\infty(x,t)| \sim U_0 \exp[-(x/a)\sqrt{\omega/2}], \quad \omega \gg l^2, \qquad (3.12)$$

$$|\mathcal{U}_\infty(x,t)| \approx U_0 \exp[-x(a\omega)^2/(2c^3)], \quad \omega \ll l^2, \qquad (3.13)$$

Thus, it is clear that $|\mathcal{U}_\infty|$ is a decreasing function of frequency and that for a fixed value of x and small values of ω, it is of a Gaussian nature with respect to frequency.
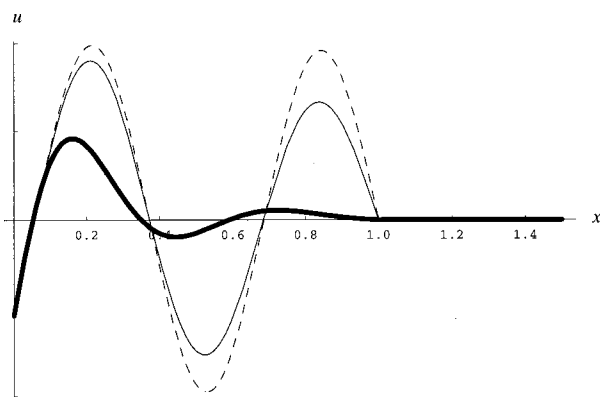

FIG. 4. u vs x (ND) for $t=c=1.0$ and $\omega=10.0$. Bold line: $r=10.0$; solid line: $r=1.0$; and broken line: $r=0.1$.
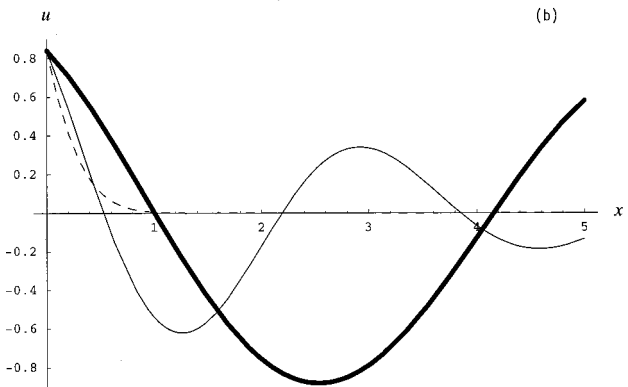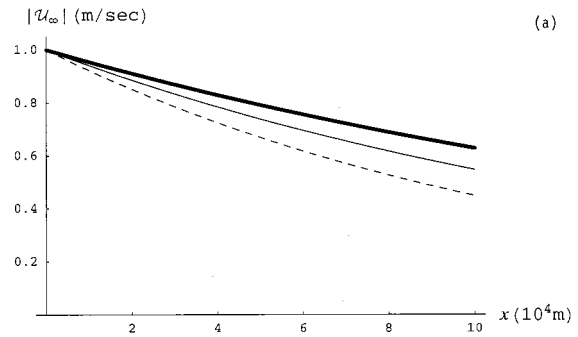

FIG. 5. (a) $|\mathcal{U}_\infty|$ vs x for dry air with $\mu=1.7\times10^{-5}$ Pa sec, $\rho_0 = 1.293$ kg/m³, and $\omega=5.0$ kHz. Bold line: $c=361.0$ m/sec; solid line: $c=331.0$ m/sec; and broken line: $c=301.0$ m/sec. (b) u vs x (ND) for $t=0.1$ and $\omega=10.0$. Bold line: $c=10.0$; solid line: $c = 5.0$; and broken line: $c=0.05$.

Last, from the $a>0$, $g(t)=U_0 \sin(\omega t)$ case of Eq. (2.6) we obtain, based on the initial condition $u(x,0)=0$, the integral relation

$$\frac{\omega}{\pi}\int_0^\infty \frac{\sin[x(\eta+l^2)/\sqrt{\eta a^2}]d\eta}{(\eta+l^2)^2+\omega^2}$$
$$= e^{-\alpha_1 x}\sin(\alpha_2 x) \quad (a,c>0;x,\omega \geq 0). \qquad (3.14)$$

This definite integral does not appear in any reference that we are aware of [19,20]. Thus, to the best of our knowledge, the relation given in Eq. (3.14) is a new result.

IV. NUMERICAL RESULTS

Here we give *Mathematica* [20]-generated plots for various values of time and the solution parameters. So as to simplify their presentation and comparison, we have, in Figs. 3, 4, 5(b), and 8, employed the following nondimensional (ND) transformations:

$$x'\rightarrow xl^2 U_0^{-1}, \quad t'\rightarrow tl^2, \quad u'\rightarrow uU_0^{-1}, \quad \omega'\rightarrow\omega l^{-2},$$
$$c'\rightarrow cU_0^{-1}, \quad a'\rightarrow c', \quad r'\rightarrow rl^{-2}, \qquad (4.1)$$

where in referring to these quantities the primes will be understood. Moreover, with the exception of Fig. 5(a), the val-
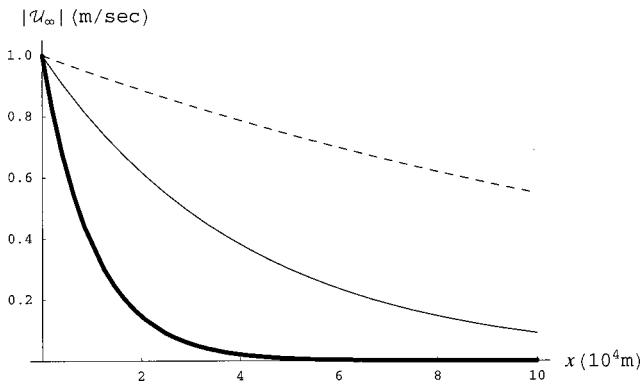
FIG. 6. $|\mathcal{U}_\infty|$ vs x for air at 0 °C. Bold line: $\omega = 20.0$ kHz; solid line: $\omega = 10.0$ kHz; and broken line: $\omega = 5.0$ kHz.

FIG. 8. ω vs α_2 (ND) for $c = 1.0$.

ues employed for all physical parameters were obtained from Ref. [1] [Table (b), p. 462]. (In particular, for air at 0 °C we have $\mu = 1.7 \times 10^{-5}$ Pa sec, $\rho_0 = 1.293$ kg/m^3, and $c = 331.6$ m/sec). Lastly, in all dimensional figures we have taken $U_0 = 1$ m/sec and, with the exceptions of Figs. 5(a), 6, and 8, all graphs given in this section were plotted for $g(t) = \sin(\omega t)$.

A. Effects of damping coefficients

In Fig. 3 we have plotted both the hyperbolic (bold line) and classical (solid line) solution curves for $c = r = 1.0$ using ND units. Clearly, the damping effects of the mixed derivative term are more pronounced than those of the usual first-order time derivative damping term occurring in the hyperbolic equation. In Fig. 4 we show the effects of varying r (>0) in Eq. (2.6), again using ND units. As would be expected, increasing r drives down the curve's amplitude and suppresses its oscillatory behavior.

B. Effects of the phase speed parameter and frequency

As is well known in the hyperbolic formulation the constant c is the phase speed (i.e., the speed at which the wave front propagates). However, in the classical formulation c takes on a totally different physical meaning. (Kinsler *et al.* [1] also note this point and refer to c as the thermodynamic speed of sound in the classical case.) From Figs. 5 we see that in the classical case, c acts like an inverse decay parameter (i.e., increasing c beyond unity decreases the decay rate
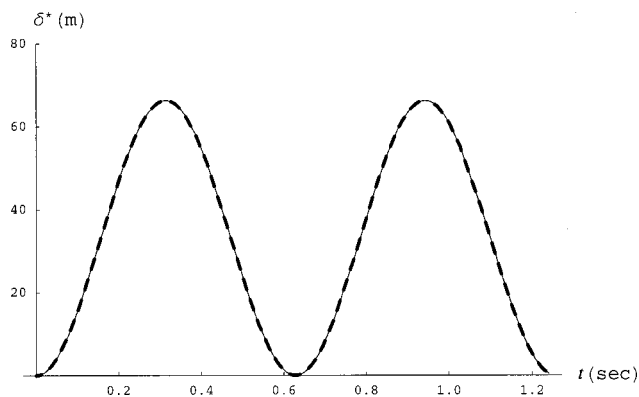

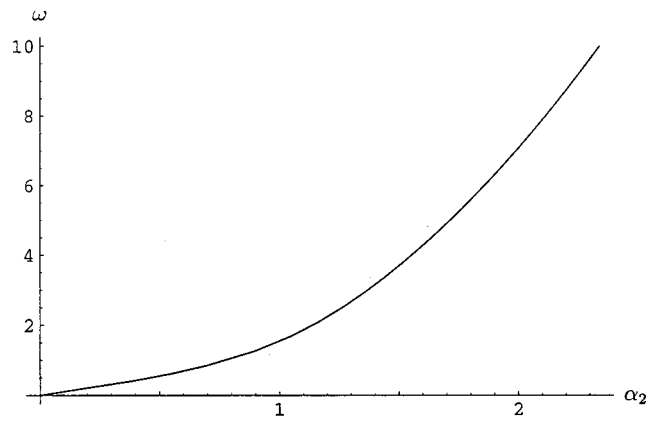FIG. 7. δ^* vs t for air at 0 °C with $\omega = 10.0$ Hz. Bold broken line: hyperbolic; solid line: classical.

of the diffusive curve). This behavior is clearly seen in the $|\mathcal{U}_\infty|$ vs the x graph shown in Fig. 5(a) which was plotted for dry air at 50.0 °C (bold line), 0 °C (solid line), and -50.0 °C (broken line) (see Pierce [21] [Eq. (1-9.4)]), and t large; and in the u vs x (ND) graph of Fig. 5(b) which was plotted for $t = 0.1$. Furthermore, we note that the broken curve shown in Fig. 5(b), plotted for $c = 0.05$, approximates the solution curve of the ND heat equation [i.e., letting $c \to 0^+$ in Eq. (1.4)] for the corresponding IBVP.

In Fig. 6 we have plotted, again for air at 0 °C, $|\mathcal{U}_\infty| = e^{-x\alpha_1}$ vs x for $\omega = 20.0$ kHz (bold line), 10.0 kHz (solid line), and 5.0 kHz (broken line). As supported by Eqs. (3.11) and (3.12), $|\mathcal{U}_\infty|$ is obviously a decreasing function of frequency.

C. Displacement thickness and dispersion relation

Figure 7 depicts δ^* vs t under the classical (solid line) and hyperbolic (bold broken line) cases. Observe that both curves appear to be in phase, non-negative, and nearly identical in amplitude.

The ND plot shown in Fig. 8 is a Brillioun diagram [18]. The mapping of the wave number to ω it depicts is known as a dispersion relation. Geometrically, the slope of the vector from the origin to a particular point on the curve represents the phase velocity v_p. From Fig. 8 we see that, since $v_p > 0$, $\mathcal{U}_\infty$ is a disturbance that always propagates away from the plate into the fluid medium. Furthermore, it is also clear that v_p is an increasing function of ω. Hence the propagation medium considered here is one of anomalous dispersion.

D. Physical scenario

Consider a very deep, initially queasiest, volume of ocean filling the half-space $x > 0$ of a Cartesian coordinate system. As a result of an undersea seismic event, a very large flat section of the ocean floor (i.e., assumed to be of infinite extent), which occupies the yz plane, begins to suddenly execute small-amplitude vibrations of the form $\sin(\omega t)$ in the vertical direction (i.e., along the x axis) at $t = 0^+$. These vibrations of the ocean floor sets the water above into motion. We wish to describe, for any $t > 0$ and neglecting gravitational effects, the resulting velocity field of the water given that flow parallel to the yz plane (i.e., flow emanating from the edges) will be negligibly small compared to that parallel to the x axis, thus allowing us to take $\mathbf{v} = (u(x,t),0,0)$.

Figures 9 were generated for $a^2 = 4\mu/(3\rho_0)$ and $r = 4\mu\omega^2/(3\rho_0 c^2)$, where the values of ρ_0, c, and μ corresponding to seawater at 13 °C were used [1]. The sequence shown compares the time evolution of the hyperbolic solution of the above scenario to that of the classical case for a vibration frequency of $\omega = 10$ Hz. Clearly, the wave front associated with the hyperbolic formulation is propagating with finite speed and is attempting to ''catch up'' to the diffusive curve. For its part, the diffusive ''wave front'' has instantly propagated over the entire positive x axis. It is therefore apparent that the approximate hyperbolic formulation suggested by McLachlan [7] is a more realistic model of the above physical problem, in terms of causality, than is the classical formulation.

V. CLOSURE

A. Conclusions

Based on the analysis given here and the values of the parameters considered, we give the following conclusions.

(1) Under the classical form of the problem $(a>0)$, u is always of a diffusive nature. Hence, a boundary input will instantly, but unequally, be felt throughout the entire half-space $x>0$.

(2) Under the hyperbolic approximation of the problem $(r>0)$, u is always of a wavelike nature; a boundary input will propagate into the half-space at the finite speed $c>0$.

(3) The physical meaning of the constant c is different in the two formulations. In the diffusive case it acts as an inverse decay parameter while for the hyperbolic case it is the speed at which a boundary input is propagated into the solution domain (i.e., the phase speed).

(4) Under the hyperbolic formulation, for $g(t) = U_0 \sin(\omega t)$, u is continuous, while possessing a corner, but u_x and u_t both suffer finite jumps across the plane $x = ct$. In contrast, taking $g(t) = U_0 \cos(\omega t)$ results in u itself experiencing a finite jump across $x = ct$. (See Table I and also Fig. 2.) Thus, for $g(t) = U_0 \cos(\omega t)$ the plane $x = ct$ is a shock wave while for $g(t) = U_0 \sin(\omega t)$ it is an acceleration wave [16].

(5) For a given value of time, the displacement thickness δ^* is proportional to the coefficient a for the $a>0$ case of Eq. (2.6) while for the $r>0$ case, δ^* is proportional to the phase speed c.

(6) For $\omega \gg l^2$, the diffusive sustained solution u_∞ takes on the character of the solution to the heat or equation. For $\omega \ll l^2$, u_∞ approximates the sustained part (i.e., nonintegral term) of the $r>0$ case of Eq. (2.6) where $r = 4\mu\omega^2/(3\rho_0 c^2)$, thus validating the derivation of Eq. (1.6). When ω is so small so that ω^2 can be neglected compared to ω, we find that both u_∞ and the sustained part of the $r>0$ case of Eq. (2.6) behave like $g(t-x/c)$, a solution of the classic wave equation.

(7) For $g(t) = U_0 \cos(\omega t)$, both the diffusive and hyperbolic solutions are independent of ω under small-time conditions. This is not the case for $g(t) = U_0 \sin(\omega t)$.

(8) For $a>0$, the propagation medium considered here is one of anomalous dispersion (see Fig. 8). However, when $\omega \ll l^2$ or $0 < r \ll 2c/x$, the propagation medium behaves in essentially a nondispersive manner (i.e., as if both a and r were negligibly small).
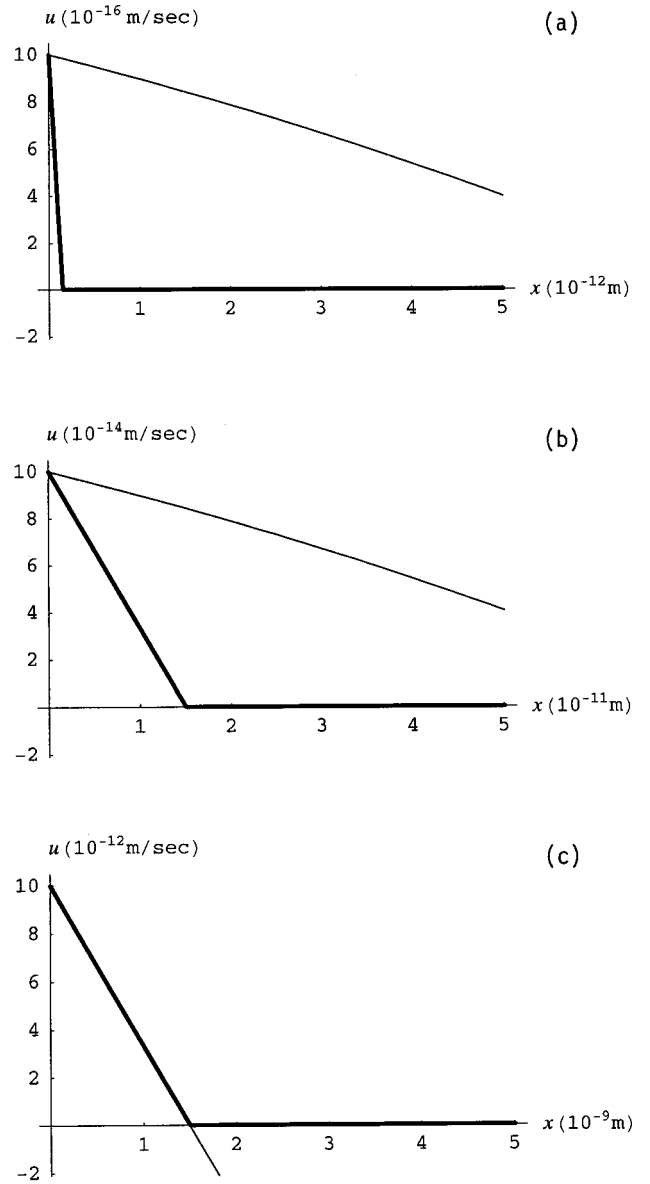
FIG. 9. u vs x for $\rho_0 = 1026.0$ kg/m^3, $c = 1500.0$ m/sec, $\mu = 0.001$ Pa·sec, and $\omega = 10.0$ Hz. Bold, hyperbolic [$r = 4\mu\omega^2/(3\rho_0 c^2)$]; solid, classical [$a^2 = 4\mu/(3\rho_0)$]. (a) $t = 10^{-16}$ sec, (b) $t = 10^{-14}$ sec, and (c) $t = 10^{-12}$ sec.

(9) The modulus of the complex diffusive sustained solution, $|\mathcal{U}_\infty|$, is a decreasing function of ω (see Figs. 5). For x fixed and $\omega \ll l^2$, $|\mathcal{U}_\infty|$ is of a Gaussian nature with respect to ω while for $\omega \gg l^2$ it approximates the corresponding solution of the classic diffusion equation.

B. Discussion

The analysis presented here clearly indicates that the approximate, hyperbolic formulation of this problem clearly results in a more realistic model of this physical system than does the classical formulation based on the linearized continuity, Navier-Stokes, and state equations. In particular, solutions of the hyperbolic equation of motion clearly satisfy causality; the smooth, diffusive solutions of the classical theory do not. Also, the positive constant c is correctly associated with the phase speed in the hyperbolic case whereas in the classical case it acts as an inverse decay parameter.

Moreover, the hyperbolic equation used here is also employed in place of the well-known heat equation, which also suffers from an infinite propagation speed defect, in heat transfer problems involving very low temperatures and/or high heat flux conditions [8]. It is of interest to note that the problem considered here has a simple mechanical analogy. It consists of a semi-infinite, one-dimensional string, initially at rest and laying on the positive x axis, with either internal ($a > 0$) or external ($r > 0$) damping [4]. At $t = 0^+$ the string's end point at $x = 0$ begins to execute transverse oscillations of the form $g(t)$. From the analysis presented here, we would be forced to conclude that the oscillations induced at $x = 0$ would be felt instantly, but unequally, at all points of an internally damped string. In contrast, for a string with only external damping, the oscillations induced at the boundary would propagate along the positive x axis, away from the plane $x = 0$, at the constant (finite) speed c.

Lastly, we call attention to the following. The classical equation of motion studied here arises from the assumption that the fluid medium (e.g., air, water) it is describing is, mathematically, a continuum. In contrast, the hyperbolic equation is, in its many applications, derivable from discrete consideration (e.g., phonons in a thermally conducting medium [8], schools of fish [10], and random walk problems [11]). Note, however, as pointed out in Sec. I, that with the appropriate coefficients both Eqs. (1.4) and (1.6) also describe the motion of certain types of linear viscoelastic flu-

ids, the former being associated with the Kelvin-Voigt body theory while the latter results from the Maxwell body model [5,22]. In particular, we call attention to the fact that a damped wave equation is the exact equation of motion for a linear Maxwellian fluid [5,22,23] (implying that all causal requirements are automatically satisfied in well-posed IB-VP's). Therefore, based on the analysis presented here, one can conclude that linear isothermal, compressible viscous fluids [i.e., those described by Eq. (1.4) under the classic theory], may be better characterized, at least in terms of causality, as linear viscoelastic fluids of the Maxwell type [5,22–25]. Furthermore, we call attention to both the theoretical and experimental results suggesting that air does in fact possess the general characteristics of such a viscoelastic fluid (see Ref. [23], Chap. 6 and the references therein).

ACKNOWLEDGMENTS

[1] L. E. Kinsler *et al.*, *Fundamentals of Acoustics*, 3rd ed. (Wiley, New York, 1982).

[2] D. T. Blackstok, J. Acoust. Soc. Am. **41**, 1312 (1967).

[3] F. R. Norwood, J. Acoust. Soc. Am. **44**, 450 (1968).

[4] R. B. Guenther and J. W. Lee, *Partial Differential Equations of Mathematical Physics and Integral Equations* (Dover, New York, 1996), pp. 206–208.

[5] A. M. Freudenthal and H. Geiringer, in *Handbuch der Physik*, edited by S. Flügge (Springer-Verlag, Berlin, 1958), Vol. 6, pp. 229–433.

[6] F. M. White, *Viscous Fluid Flow*, 2nd ed. (McGraw-Hill, New York, 1991), pp. 138–141.

[7] N. W. McLachlan, *Modern Operational Calculus* (Macmillan, London, 1948), pp. 71–74.

[8] D. D. Joseph and L. Preziosi, Rev. Mod. Phys. **61**, 41 (1989); **62**, 375 (1990).

[9] M. Born and E. Wolf, *Principles of Optics*, 3rd ed. (Pergamon Press, London, 1965), pp. 611–615.

[10] H.-S. Niwa, J. Theor. Biol. **193**, 215 (1998).

[11] S. Goldstein, Q. J. Mech. Appl. Math. **4**, 129 (1951).

[12] P. M. Morse and H. Feshbach, *Methods of Theoretical Physics* (McGraw-Hill, New York, 1953), p. 137.

[13] J. S. Toll, Phys. Rev. **104**, 1760 (1956).

[14] P. M. Jordan and A. Puri, J. Appl. Phys. **85**, 1273 (1999).

[15] R. V. Churchill, *Operational Mathematics*, 3rd ed. (McGraw-Hill, New York, 1972).

[16] C. Truesdell and R. A. Toupin, in *Handbuch der Physik*, edited by S. Flügge (Springer-Verlag, Berlin, 1960), Vol. 3, Pt. 1, pp. 226–793.

[17] A. L. Fetter and J. D. Walecka, *Theoretical Mechanics of Particles and Continua* (McGraw-Hill, New York, 1980), pp. 413–415.

[18] W. C. Elmore and M. A. Heald, *Physics of Waves* (Dover, New York, 1985), pp. 122–127.

[19] I. S. Gradshteyn and I. M. Ryzhik, *Tables on Integrals, Series, and Products*, 5th ed., edited by A. Jeffrey (Academic, San Diego, 1994).

[20] S. Wolfram, *The Mathematica Book*, 4th ed. (Wolfram Media/Cambridge University Press, New York, 1999).

[21] A. D. Pierce, *Acoustics: An Introduction to its Physical Principles and Applications* (Acoustical Society of America, New York, 1989), p. 29.

[22] M. Reiner, in *Handbuch der Physik*, edited by S. Flügge (Springer-Verlag, Berlin, 1958), Vol. 6, pp. 434–550.

[23] A. G. Fredrickson, *Principles and Applications of Rheology* (Prentice-Hall, New York, 1964).

[24] J. L. Leander, J. Acoust. Soc. Am. **100**, 3503 (1996).

[25] J. L. Leander, J. Acoust. Soc. Am. **94**, 1643 (1993).